

ORIGIN OF π -FACIAL DIASTEREOSELECTION IN CARBONYL ADDITION. APPLICATION OF THE EXTERIOR FRONTIER ORBITAL EXTENSION MODEL TO 1,3-DIHETERAN-5-ONES (HETEROATOM = O, S)

Shuji Tomoda*, Daisuke Kaneno, and Takatoshi Senju

Department of Life Science, Graduate School of Arts and Sciences
The University of Tokyo, Komaba, Meguro-ku, Tokyo 153-8902, Japan
(e-mail : tomoda@selen.c.u-tokyo.ac.jp)

Abstract- The exterior frontier orbital extension model (the EFOE Model) strongly suggested that reversal of π -facial diastereoselection in nucleophilic additions of 1,3-diheteran-5-ones (heteroatom = O or S) may originate from the unique ground-state conformation and the π -facial difference in the LUMO extension around the carbonyl carbon rather than from transition state effects. Intrinsic reaction coordinate (IRC) and natural bond orbital (NBO) analyses of transition states of LiAlH_4 reduction of these ketones have strongly indicated that the transition state effects (the torsional strain of the ketone moieties and the antiperiplanar effects involving the incipient bond proposed by the conventional theoretical models for π -facial diastereoselection; the Felkin-Anh model and the Cieplak model) are not responsible for facial selection.

The origin of π -facial diastereoselection of addition reactions to unsaturated organic substrates has recently attracted active debate.¹ Since Cieplak's proposal of his conceptual model in 1981,² most discussions are focused on the importance of transition state stabilization mechanisms arising from the antiperiplanar hyperconjugative stabilization effect involving the incipient bond (hereafter abbreviated as 'the AP effect') and/or from the torsional strain of substrate.^{3,4} Resolution between the two opposite mechanisms of the AP effect known as the Felkin-Anh model⁴ and the Cieplak model² has been the subject of intense investigation for these two decades (Figure 1). While the former model assumes an electron-rich transition state,⁴ the latter postulates an electron-deficient incipient bond in common organic reactions.² As a consequence, most arguments are based on the transition state stabilization effects. Nevertheless they have rarely been evaluated quantitatively.

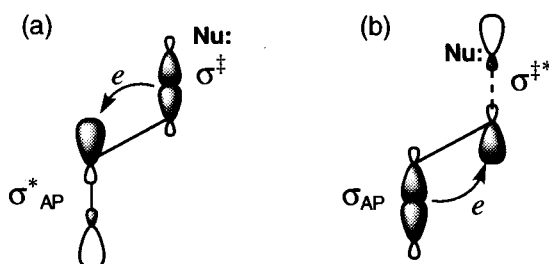
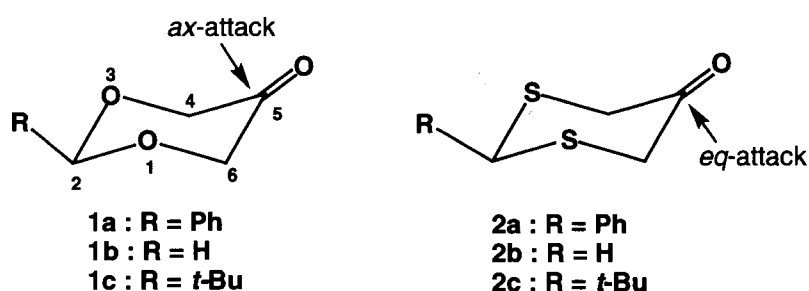


Figure 1. Mechanisms of the antiperiplanar hyperconjugation effects in conventional transition state models. (a); Felkin-Anh model.⁴ (b); Cieplak model.² (Nu: = nucleophile)

Recently we have shown⁵ that the transition state effects, such as torsional strain and the AP effects, are not essential for π -facial diastereoselection of nucleophilic additions to cyclic ketones including cyclohexanone,⁶ 3- or 4-substituted cyclohexanones⁷ and 5-substituted adamantan-2-ones⁸ using the transition states of the reduction with LiAlH_4 . Although it was found that the incipient bond is electron-deficient, showing the predominance of the Cieplak effect over the Felkin-Anh effect, surprisingly they often operate *against* observed facial stereoselectivity in many cyclic ketones including adamantan-2-ones. In particular, it was strongly suggested by intrinsic reaction coordinate (IRC) analysis as well as Weinhold's natural bond orbital (NBO) analysis⁹ of the LiAlH_4 reduction of cyclohexanone that the AP effects should be stronger in the equatorial hydride attack than in the axial process. To this end we have recently proposed a new theoretical model called 'the exterior frontier orbital extension model (the EFOE Model)' based on the simple assumption that the ground-state properties of unsaturated substrates (ketones) should be responsible for facial diastereoselection.¹⁰ Remarkable predictive power of this simple model constructed according to the Salem-Klopman driving force equation¹¹ has been shown in numerous examples of hydride reductions and MeLi addition reactions of a variety of cyclic carbonyl substrates.⁵ Herein we shall describe further successful application of the theoretical approach using 1,3-diheteran-5-ones (heteroatom = O, S; **1** and **2**), the facial diastereoselection of which has been a long-standing puzzle.



The unique reversal of face selection in nucleophilic carbonyl additions of 2-phenyl-1,3-dioxan-5-one (**1a**) and 2-phenyl-1,3-dithian-5-one (**2a**) has been a controversial debate since early 1980.² Jochims *et al.* reported LiAlH_4 reduction of **1a**.¹² The product ratio of the equatorial and axial alcohol was 94 : 6, indicating slightly higher axial selectivity than 4-*tert*-butylcyclohexanone (ax : eq = 92 : 8).¹³ Surprisingly, in sharp contrast to the behavior of cyclohexanone, the Grignard reaction of **1a** afforded almost exclusive equatorial alcohol *via* axial attack (ax-attack) (96–98%) even when bulky reagents, such as *iso*-PrMgI or *tert*-BuMgI, were employed. Jochims interpreted these unusual results in terms of reduced steric hindrance in the axial face of **1a** owing to the lack of two axial hydrogens at the 1- and 3-positions in the 6-membered ring. Interestingly, their subsequent studies using the sulfur analog (**2a**) indicated complete stereochemical reversal in nucleophilic additions of **2a** with LiAlH_4 and Grignard reagents (85–93%).¹⁴

Wu and Houk reported MM2 force field calculations of the parent compounds (**1b** and **2b**). They proposed the torsional strain to be responsible for the observed stereochemistry.¹⁵ Cieplak interpreted these results according to his assumption of the order for the electron-donating abilities of the antiperiplanar bonds ($\text{C-S} > \text{C-H} > \text{C-C} > \text{C-O}$).² Wu and Houk disclosed criticism against Cieplak's hypothesis to propose again the torsional strain model combined with strong emphasis on the electrostatic solvent interaction with heteroatoms.¹⁶ Based on *ab initio* molecular orbital calculations and the exterior frontier orbital extension model, we show theoretical evidence which strongly supports our previous conclusions on the facial diastereoselection of cyclohexanone reduction.⁶

RESULTS AND DISCUSSION

Transition State Analysis

1. Structures

Figures 2 and 3 show the transition state (TS) structures for the reduction of **1b** and **2b** with LiAlH_4 calculated at the B3LYP/6-31+G(d) level. Table 1 shows some selected structural parameters along with those of cyclohexanone for comparison. The imaginary frequencies of the equatorial transition states (*eq*-TS) for **1b** and **2b** ($\nu_i = -290.7$ and -234.6 cm^{-1} , respectively) are greater than the corresponding values of the axial transition states (*ax*-TS) ($\nu_i = -340.3$ and -383.3 cm^{-1} , respectively). Each vibrational mode corresponds to the stretching vibration of the incipient bond. The overall structures around the reaction center are similar to those of cyclohexanone reduction with LiAlH_4 .⁶ For example, comparison between the TS data of the 1,3-diheteran-5-ones (**1b** and **2b**) and cyclohexanone reveals that (1) the hydride approaching angles (θ) and the torsion angles between the incipient bond and the vicinal antiperiplanar bond (the AP bond) (ϕ) are nearly the same, but (2) the incipient bond distances ($\text{C}=\text{O} \cdots \text{H}$) are much longer ($1.716 \sim 1.952 \text{ \AA}$) except for the equatorial transition state (*eq*-TS) of **2b** (1.544 \AA). These structural features suggest somewhat *earlier* transition state in **1b** and **2b** than in cyclohexanone.

Table 1. Selected structural parameters for the transition states (TS) of 1,3-diheteran-5-ones (**1b** and **2b**; X = O, S) and cyclohexanone reduction with LiAlH_4 (B3LYP/6-31+G(d))^a

Compounds	TS	ν_i^b	θ^c	$\text{C}=\text{O} \cdots \text{H}^d$	ϕ^e	H-Al	O \cdots Li	C=O	$\text{C}=\text{O}-\text{C}_\alpha$	$\text{C}_\alpha-\text{X}_\beta$
1b	<i>ax</i>	-290.7	108.6	1.862	177.2	1.660	1.822	1.254	1.525	1.419
	<i>eq</i>	-340.3	109.0	1.716	152.1	1.688	1.796	1.258	1.536	1.434
2b	<i>ax</i>	-234.6	106.4	1.952	177.3	1.652	1.830	1.252	1.524	1.829
	<i>eq</i>	-383.3	110.0	1.544	167.2	1.720	1.770	1.243	1.535	1.842
cyclohexanone ⁶	<i>ax</i>	-377.7	109.8	1.531	177.6	1.709	1.764	1.284	1.531	1.536
	<i>eq</i>	-392.6	109.5	1.556	161.6	1.702	1.771	1.283	1.530	1.547

^a Angles in degree and bond distances in \AA . ^b Imaginary vibrational frequency (cm^{-1}). ^c The angle between the incipient bond and the carbonyl bond. ^d Distance of the incipient bond. ^e The torsion angle between the incipient bond and the vicinal antiperiplanar bond.

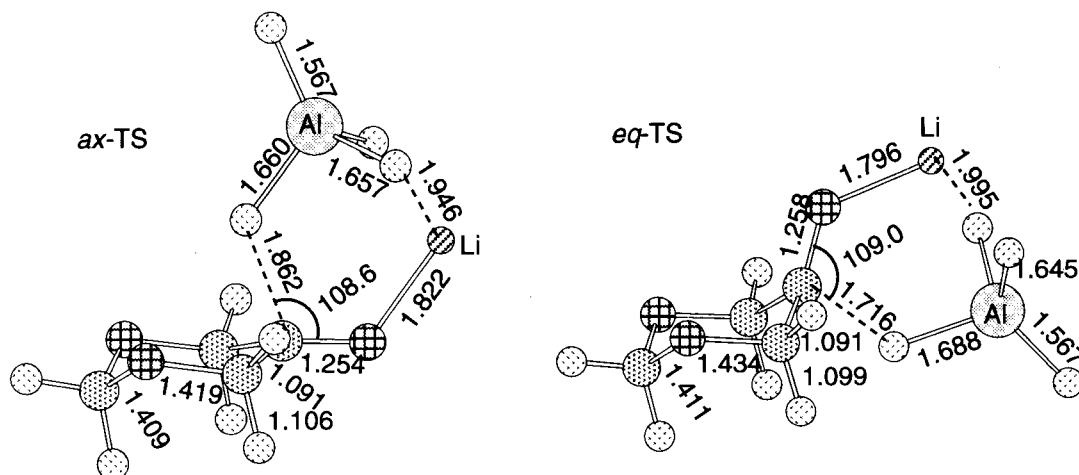


Figure 2. Transition state structures of LiAlH_4 reduction of 1,3-dioxan-5-one (**1b**) (B3LYP/6-31+G(d)). Bond lengths are in \AA and angles are in degree.

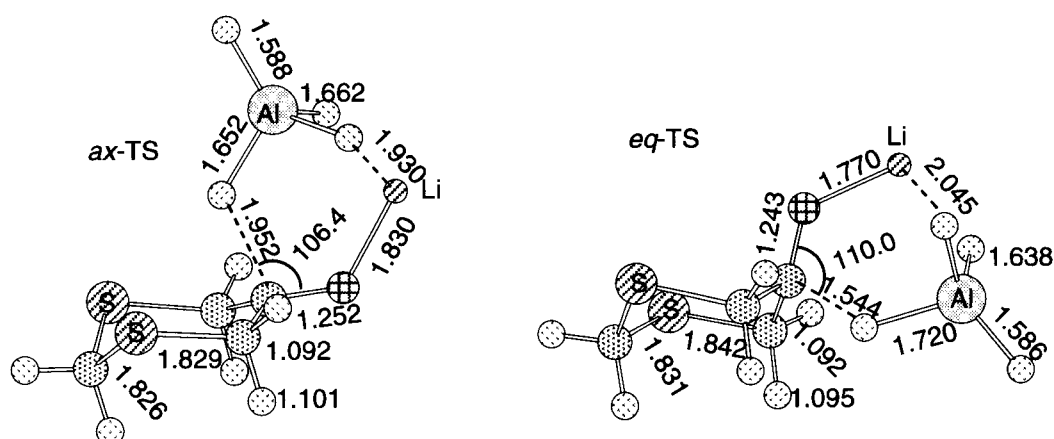


Figure 3. Transition state structures of LiAlH_4 reduction of 1,3-dithian-5-one (**2b**) (B3LYP/6-31+G(d)). Bond lengths are in Å and angles are in degree.

Table 2 shows the results of vibrational analysis. Relative ZPVE(zero point vibrational energy)-corrected total electronic energies between the axial transition state (*ax*-TS) and the equatorial one (*eq*-TS) for **1b** and **2b** were 2.44 and $-2.06 \text{ kcal mol}^{-1}$, respectively, in agreement with the experimental stereoselectivity for **1a** and **2a**.

Table 2. Vibrational analysis of the transition states (TS) for LiAlH_4 reduction of 1,3-diheteran-5-ones (**1b** and **2b**).^a

Compds	TS	freq. ^b	ZPVE ^c	E^d	ΔE^e	$\Delta\Delta H^\ddagger^f$	$\Delta\Delta G^\ddagger^g$
1b	<i>ax</i>	-290.7	83.75	-634.077257	2.44	2.68	2.62
	<i>eq</i>	-340.3	83.96	-634.073362			
2b	<i>ax</i>	-234.6	78.97	-1280.023831	-2.06	-1.67	-1.39
	<i>eq</i>	-383.3	79.42	-1280.027120			

^a Calculated at the B3LYP/6-31+G(d) level. ^b Imaginary vibrational frequency in cm^{-1} . ^c Zero point vibrational energy in kcal mol^{-1} . ^d Total electronic energy in atomic unit ($627.5084 \text{ kcal mol}^{-1}$). ^e $\Delta E = E_{\text{eq}} - E_{\text{ax}}$ in kcal mol^{-1} . ^f $\Delta\Delta H^\ddagger = H_{\text{eq}} - H_{\text{ax}}$ ($H = E + RT$; $T = 298.15 \text{ K}$) in kcal mol^{-1} . ^g $\Delta\Delta G^\ddagger = G_{\text{eq}} - G_{\text{ax}}$ ($G = H - TS$; $T = 298.15 \text{ K}$) in kcal mol^{-1} .

2. Transition State Stabilization Effects

The torsional strain analysis of the LiAlH_4 TS of cyclohexanone at the B3LYP/6-31+G(d) level has previously provided strong theoretical evidence against the torsional strain model.⁵ The transition state analyses of the model compounds (**1b** and **2b**) further supports this conclusion. The difference in the total electronic energy of the bare 6-membered ring moiety (distorted 1,3-diheteran-2-one moiety) between *ax*-TS and *eq*-TS was found to be $5.89 \text{ kcal mol}^{-1}$ for **1b** and $4.06 \text{ kcal mol}^{-1}$ for **2b** (MP2/6-31+G(d)), indicating that the torsional strain is greater in *eq*-TS than in *ax*-TS in *both* cases. Substantially greater deformation of the 6-membered ring in *eq*-TS of **2b** ($4.06 \text{ kcal mol}^{-1}$) is surprising because this is not consistent with the observed facial stereoselection of **2a**.¹⁴ This clearly indicates that there is no logical basis to single out the torsional strain of the substrate ketone moiety alone to discuss π -facial diastereoselection.

Theoretical evidence against the Cieplak model has been obtained by computing the magnitude of the antiperiplanar bond elongation as well as by natural bond orbital (NBO) analysis.⁹ As shown in Table 3, the

LiAlH₄ transition states of **1b** show significant difference in percent bond elongation (%BE)¹⁷ of the antiperiplanar bonds vicinal to the incipient bond (C4–H_{4ax}/C6–H_{6ax} for *ax*-TS or C4–O3/C6–O1 for *eq*-TS) due to the antiperiplanar hyperconjugative stabilization effect (hereafter called "the AP effect") between the *ax*-TS (+0.11%) and *eq*-TS (+0.62%) relative to the ground-state **1b** optimized at the same level. The relative magnitude of these AP effects is clearly inconsistent with the observed facial selection for **1a**.^{12,14} In consonant with these results, the difference in NBO bond population⁹ for the antiperiplanar bonds between the transition state and the ground state (Δ BP) was $-0.0068 e$ (electrons) for *ax*-TS and $-0.0081 e$ for *eq*-TS. The greater Δ BP for the latter is again consistent with the greater AP effect in *eq*-TS. Consequently, neither the Cieplak model² nor the Felkin-Anh model⁴ can be employed to explain the observed facial diastereoselection for **1**.

Exactly the same arguments can be made for the sulfur analog (**2b**). The percent elongation (%BE)¹⁷ of the vicinal antiperiplanar bonds (C4–H_{4ax}/C6–H_{6ax} for *ax*-TS or C4–S3/C6–S1 for *eq*-TS) for *ax*-TS and *eq*-TS for **2b** were +0.25% and -0.11% , respectively. It should be particularly noted that the C–S bonds are *shortened* in the more stable *eq*-TS compared with those of the ground state substrate! The values of Δ BP for the antiperiplanar bonds, calculated for the LiAlH₄ transition states of **2b**, were $-0.0188 e$ for *ax*-TS and $-0.0002 e$ for *eq*-TS. Hence, the AP effects are clearly operating against observed diastereoselectivities both in **1b** and **2b** as found in the case of cyclohexanone reduction.⁶ The relative magnitude of the transition state AP effects (*ax*-TS *vs.* *eq*-TS) for both **1b** and **2b** clearly indicate that if the AP effects were the major mechanism of facial stereoselection, stereoselectivity opposite to the experimental result must be observed, contrary to the predictions of both conventional models.^{2,4} We emphasize here again that *the AP effects should be regarded merely as a major internal (intramolecular) energy relaxation mechanism that operates against the direction of the bond formation process.*

Table 3. Tridentate transition state structures and antiperiplanar effects for LiAlH₄ reduction of 1,3-diheteran-5-ones (**1b** and **2b**) (Heteroatom (X) = O or S) calculated at the B3LYP/6-31+G(d) level.^a

X	TS	θ^b	ϕ^c	τ^d	C5...H ^e	C5=O	C4–H _{ax} (C6–H _{ax})		C4–X3 (C6–X1)	
							(Å)	BP ^g	(Å)	BP ^g
							(%BE) ^f	(Δ BP) ^h	(%BE) ^f	(Δ BP) ^h
O	<i>ax</i>	108.6	177.2	32.0	1.862	1.254	<u>1.106</u> (+0.11%)	<u>1.9606</u> (–0.0068)	1.419 (–0.41%)	1.9886 (–0.0001)
	<i>eq</i>	109.0	152.1	55.2	1.716	1.258	1.099 (–0.56%)	1.9842 (+0.0168)	<u>1.434</u> (+0.62%)	<u>1.9806</u> (–0.0081)
S	<i>ax</i>	106.4	177.3	42.3	1.952	1.252	<u>1.101</u> (+0.25%)	<u>1.9584</u> (–0.0188)	1.829 (–0.80%)	1.9821 (+0.0140)
	<i>eq</i>	110.0	167.2	70.3	1.544	1.243	1.095 (–0.27%)	1.9854 (+0.0082)	<u>1.842</u> (–0.11%)	<u>1.9679</u> (–0.0002)

^a Angles and bond lengths are in degree and Å, respectively. ^b Angle of hydride approach with respect to C=O bond. ^c Dihedral angle between C5...H and C5–C4 or C5–C6 bonds. ^d Dihedral angle between C4–C5 and C6–X1 bonds. ^e Distance of the incipient bond between hydride and C5. ^f Percent bond elongation (+) or shrinkage (–) relative to the corresponding bond distance of ground-state 1,3-diheteran-5-one optimized at the B3LYP/6-31+G(d) level. ^g Bond population calculated with NBO analysis at the B3LYP/6-31+G(d) level. ^h Difference in bond population of the corresponding bond between TS and ground-state 1,3-diheteran-5-one optimized at the B3LYP/6-31+G(d) level.

3. Intrinsic Reaction Coordinate (IRC) Analysis

The remarkable conclusions drawn from the above transition state analyses are further substantiated by intrinsic reaction coordinate (IRC) analyses at the B3LYP/6-31+G(d) level (except for the *eq*-TS of **1b** for which the B3LYP/6-31G(d) level was employed). Figure 4 depicts plots of % bond elongation of the antiperiplanar bonds (%BE) against the IRC. Figure 5 depicts plots of the amount of reduced bond population of the antiperiplanar bonds relative to the electron population of the corresponding bond of substrate ketone (Δ BP) against the IRC. In all cases studied, not only the AP effects (roughly) monotonically decrease toward transition states, but also they operate against observed facial stereoselection. In the reduction of **1b**, the AP effects in the process toward *ax*-TS are always smaller than those in the corresponding equatorial process. On the other hand, the less preferred axial process of the reaction of **2b** shows always much greater AP effects. It should be particularly noted that the preferred equatorial process of **2b** shows *negative* %BE almost all the way along the IRC, indicating that the antiperiplanar bonds are shorter than those in the initial substrate ketone during this process. All these theoretical observations strongly suggest the following two remarkable statements: (1) the AP effects operate effectively in the *initial* process and they are *attenuated* steadily toward the transition state and (2) they operate *against* observed facial diastereoselection.

In agreement with these conclusions, NBO analysis along the IRC toward the transition states suggested that the amount of reduced bond population of the antiperiplanar bonds relative to the electron population of the corresponding bond of substrate ketone (Δ BP) monotonically decrease along the IRC as shown in Figure 5. This again clearly suggests that the strength of the antiperiplanar bonds *increase* toward the transition state and is entirely consistent with the trends exhibited by %BE (Figure 4).

In complete accordance with our previous conclusions on similar analyses of cyclohexanone reduction with LiAlH_4 ,⁶ the two quantities (%BE and Δ BP) for the corresponding reaction of **1b** and **2b** also provide remarkable evidence against the conventional transition state models.^{2,4}

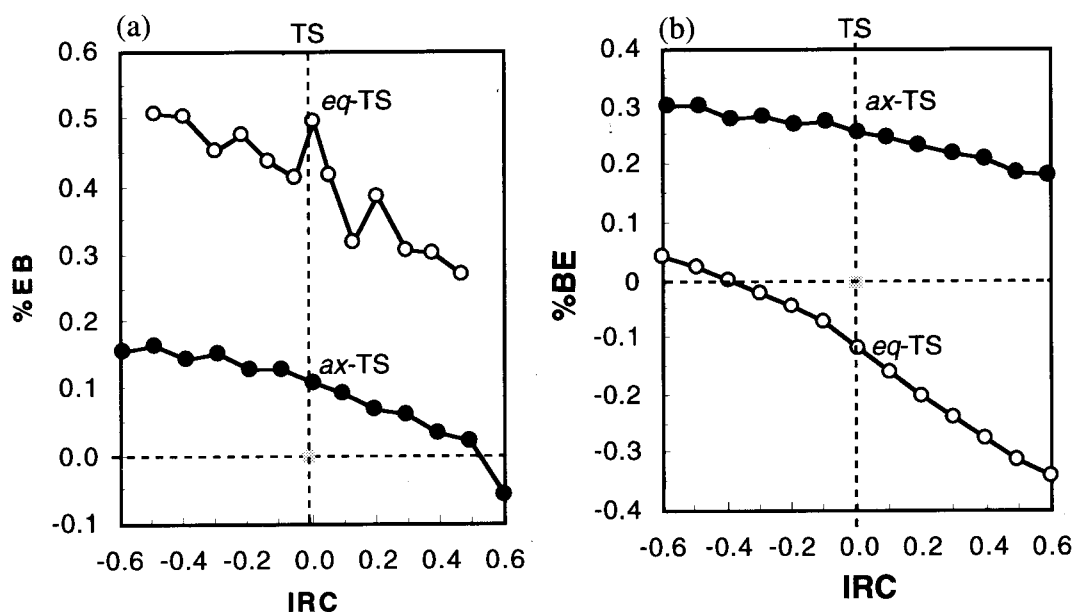


Figure 4 Plot of % elongation of the antiperiplanar bonds (%BE) against the intrinsic reaction coordinate (IRC: unit; $\text{amu}^{1/2} \text{ bohr}$) for the LiAlH_4 reduction of; (a) 1,3-dioxan-5-one (**1b**) and (b) 1,3-dithian-5-one (**2b**) (B3LYP/6-31+G(d) except for *eq*-TS of **1b** for which B3LYP/6-31G(d) was used). (Filled circles; axial process; open circles; equatorial process)

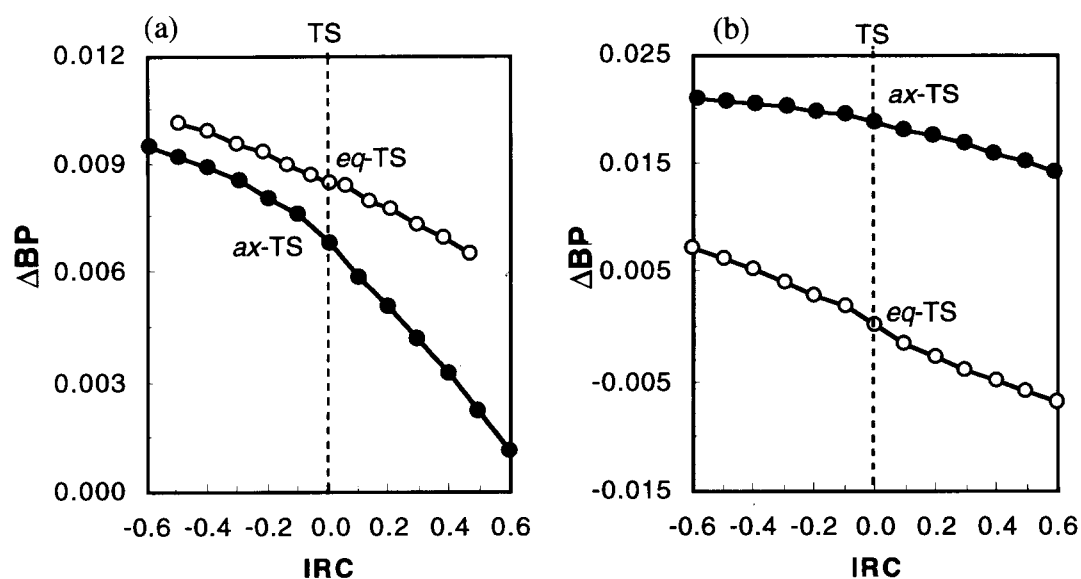
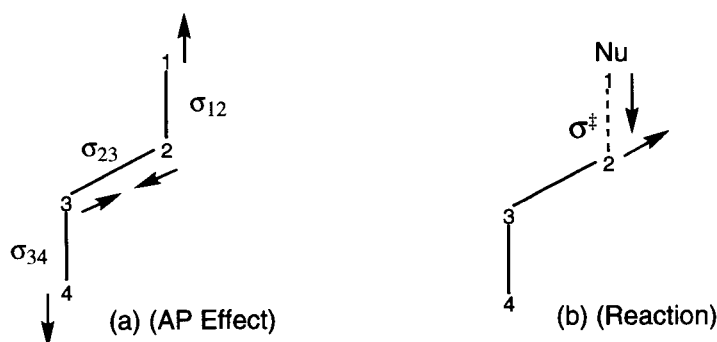


Figure 5 Plot of reduced bond population of the antiperiplanar bonds (ΔBP) against the intrinsic reaction coordinate (IRC: unit; $\text{amu}^{1/2} \text{ bohr}$) for the LiAlH_4 reduction of; (a) 1,3-dioxan-5-one (**1b**) and (b) 1,3-dithian-5-one (**2b**) (B3LYP/6-31+G(d) except for *eq*-TS of **1b** for which B3LYP/6-31G(d) was used). (Filled circles; axial process; open circles; equatorial process)

4. Reality of Antiperiplanar Effects

The readers may wonder why the AP effects operate against observed diastereoselection. Before starting discussion on the role of the AP effects, it may be worthwhile referring to the long-standing question as to whether the transition state or the incipient bond is electron-rich or electron-deficient. Feynman's electrostatic theorem,¹⁸ which states that a chemical bond is formed as a balance of electrostatic forces among two nuclei and (generally two) electrons, reveals that an incipient bond should be intrinsically electron-deficient no matter whether the reaction is electrophilic or nucleophilic. This was confirmed by the cyclohexanone reduction.⁶ It was revealed by NBO analysis and natural resonance theoretical (NRT)⁹ analysis on the LiAlH_4 transition states of cyclohexanone⁶ that the bond orders of the incipient bonds are 0.4365 and 0.4224 for *ax*- and *eq*-TS, respectively and that the incipient bonds possess 0.696 and 0.663 electrons for *ax*- and *eq*-TS, respectively. Consequently the logical basis of the Cieplak model² seems reasonable at least in terms of the electronic nature of an incipient bond and the Cieplak mode may be greater than the Felkin-Anh mode of AP effects. The problem of the Cieplak effect is, however, more serious. Frenking's first perspective is particularly noteworthy: the Cieplak mechanism is "a clear contradiction to the frontier orbital model" because an incipient bond should become stronger when electrons are donated into the antibonding orbital of that bond.¹⁹ We point out here that the AP effect operates *generally* against incipient bond formation including Anh's mode of the AP effect⁴ for the following two reasons. Let us consider the AP effect in the planar consecutive three-bond system (1-2-3-4; σ_{12} , σ_{23} and σ_{34}) (Scheme 1; (a)).

It should be noted that some electrons are removed from the bonding region of one antiperiplanar bond (σ) into the antibonding region of the other (σ^*). As a result, both σ bonds (σ_{12} , σ_{34}) cause some elongation, indicating that the force vector at nucleus 1 or 4 (indicated by arrows on atoms 1 and 4) is directed away from atoms 2 or 3. The other unignorable mechanism against bond formation process is the movement of atoms 2 and 3.



Scheme 1. Force vectors (\rightarrow) operating in (a) the antiperiplanar hyperconjugation effects (AP effect) and (b) nucleophilic addition.

The electrons moved from these bonds (σ_{12} , σ_{34}) now reside in the bonding region of the intervening bond (σ_{23}) to cause strengthening (shortening) of the bond due to some π -character leading to some stabilization of the system. During this hyperconjugation process, the force vectors operating on atoms 2 and 3 (indicated by arrows) are directed inward along the σ_{23} bond (Scheme 1; (a)). However, the addition reaction process requires exactly the opposite direction of force vectors at one of these atoms. Suppose that atom 2 is an sp^2 -hybridized reaction center (carbonyl carbon) and atom 1 is a nucleophile (Scheme 1; (b)). The hybridization of this atom changes into sp^3 as the reaction proceeds, which requires elongation of the bond between atoms 2 and 3, indicating the operation of force vectors at these atoms *against* those generated by the AP effect. These two mechanisms strongly indicate that the AP effect operates *against the direction of the reaction process*, namely *against bond formation* and hence may operate against observed π -facial stereoselection.

Another important aspect is that the magnitude of the AP effect may be initially significant, but it is gradually diminished along the reaction coordinate near the transition state for two reasons. First, as the reaction proceeds, the strength of the incipient bond increases, causing some energy rise of the antibonding ($\sigma^{\ddagger*}$) level of the incipient bond and energy reduction of its bonding (σ^{\ddagger}) level. This may cause reduction in overall antiperiplanar stabilization involving the incipient bond. Secondly, as the reaction proceeds, the hybridization of the carbonyl carbon changes from sp^2 to sp^3 . The bond length of σ_{23} therefore increases to cause inevitable reduction in the magnitude of the AP effects as the reaction approaches the transition state. Consequently it is expected that overall antiperiplanar hyperconjugation mechanisms may operate effectively in the early stages and the difference in their magnitude between the two π -faces of the carbonyl plane may be reduced monotonically, sometimes to a marginal degree or may vanish at all, toward transition state.

These theoretical results strongly suggest that the facial differences in the transition state effects do not necessarily agree with observed diastereoselectivities. Namely the transition state events that have been intensively discussed for nearly two decades do not seem essential to π -facial diastereoselection.

Theoretical Description of the EFOE Model

1. Theoretical Basis

The simplest answer to the origin of π -facial diastereoselection would be the π -facial difference in rate constants rather than transition state events. Accordingly we apply here again 'the Exterior Frontier Orbital Extension Model (the EFOE Model)'.⁵ This model assumes that the ground state conformational and the electronic properties may be responsible for the unique stereochemical reversal observed for **1a** and **2a**. The Salem-Klopman equation (Eq.1)¹¹, a simple kinetic equation which expresses the driving force of a chemical reaction by the summation of three independent terms, is the basis of the new theory. The theoretical background of this model has been described elsewhere,^{7,8,10} but brief description will be given

here for the readers' sake.

$$\Delta E = \underbrace{-\sum_{ab} (q_a + q_b)\beta_{ab}S_{ab}}_{\text{1st term}} + \underbrace{\sum_{k<l} \frac{Q_k Q_l}{r_{kl}}}_{\text{2nd term}} + \underbrace{\sum_r^{\text{occ.}} \sum_s^{\text{unocc.}} - \sum_s^{\text{occ.}} \sum_r^{\text{unocc.}} \frac{2(\sum_{ab} c_{ra}c_{sb}\beta_{ab})^2}{E_r - E_s}}_{\text{3rd term}} \quad (1)$$

q_a, q_b = electron populations in atomic orbital a or b .

β = resonance integral.

S = overlap integral.

Q_k, Q_l = total electron densities at atom k or l .

r_{kl} = distance between atoms k and l .

E_r = energy level of MO r .

c = molecular orbital coefficients.

The first term of Eq. 1 is the exchange repulsion term, which corresponds to the interactions among filled orbitals of the reactants. This term always leads to the destabilization of the system and is generally considered as steric effect in organic chemistry. The second term is the electrostatic interaction term that is especially important in ionic reactions. The third term is the donor-acceptor orbital interaction term, which should always lead to stabilization of the reacting system, and to which the frontier orbital interaction between reactants generally contributes most. Among these three terms, Salem and Klopman pointed out that the first and the third terms should be particularly important in common organic reactions.¹¹

The EFOE model also focuses on the first and the third terms of this equation. Two new quantities – π -plane-divided accessible space (PDAS) as the steric effect term and the exterior frontier orbital extension density (EFOE density) as the orbital interaction term – constitute the new model. Both quantities focus on the exterior area of a molecule.

2. π -Plane-Divided Accessible Space (PDAS)

Steric effect is commonly introduced only as a qualitative term in organic chemistry. Highly practical asymmetric syntheses have been designed through intuitive estimation of steric effects based on the size of substituents, such as A-values^{20,21} or the van der Waals radius.²² It is however often difficult to predict steric effects of π -facial selection intuitively, in particular, for substrates having complex substituents around π -bond. A simple quantity of π -facial steric effect should provide convenient means to gain clearer and more effective perception in designing organic synthesis. Described herein is the first method of π -facial steric effect calculation that is useful for common organic unsaturated substrates.

The new method focuses on three-dimensional space outside the van der Waals surface of a reactant molecule.²³ It is based on the simple assumption that the volume of the outer (exterior) space nearest to a reaction center should contain steric information of the reactant (substrate), since this volume is precisely the three-dimensional space available for a reagent to access the reaction center of the substrate. The exterior volume is calculated for two faces of π -plane separately. Figure 6 illustrates the definition of π -plane-divided accessible space (PDAS) as a reasonable quantitative measure of π -facial steric effect using formaldehyde as an example. Molecular surface is defined as an assembly of spherical atoms having the van der Waals radii.²² Integration of exterior three-dimensional space for the PDAS of the carbonyl carbon is performed according to the following conditions. If a three-dimensional point $P(x, y, z)$ outside the repulsive surface is the nearest to the surface of the carbonyl carbon (a reaction center on xz plane) (*i.e.* if

the distance between P and the van der Waals surface of the carbonyl carbon (d_C) is the shortest compared with the distances from P to other atomic surface (two d_H and one d_O) and if the point is located above the carbonyl plane ($y > 0$), the space at this point is assigned to the above-space of the carbonyl carbon.

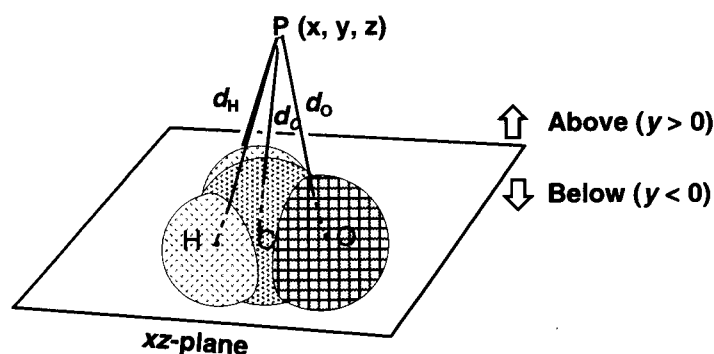


Figure 6. Definition of π -plane-divided accessible space (PDAS).

The integration (summation) of such points is defined as the PDAS of the carbonyl carbon for the above-plane. For the sake of convenience, spatial integration is limited to 5 au (2.65 Å) from molecular surface, where extension of an electronic wave function is negligible beyond this limit. In general, the carbonyl plane is defined as the plane which includes the two sp^2 atoms of the π -bond and which is parallel with the vector connecting the two atoms at the α -positions. The basic concept of PDAS definition is readily extended to other π -facial steric effect in compounds containing a general double bond other than carbonyl. The detailed calculation procedure is described in a later section.

3. Exterior Frontier Orbital Extension Density

The importance of the exterior area of a substrate in π -facial stereoselection has also been quantified by the definition of exterior frontier orbital extension density (EFOE density), which represents the third term of Eq. 1. Thus the π -plane-divided EFOE density (EFOE density) is defined as the integrated (summed) electron density of a frontier orbital (HOMO for electrophilic addition or LUMO for nucleophilic addition)²⁴ over specific exterior points over one face of the π -plane of a substrate molecule satisfying the following condition: *the absolute total value of the wave functions belonging to the carbonyl carbon makes a maximum contribution to the total value of FMO wave function at the point.* Such a condition guarantees that the driving force vector on hydride or other reagent is maximally directed toward the sp^2 reaction center. Thus integration of FMO probability density (Ψ_{FMO}^2) over such three-dimensional subspace (Ω) that satisfies the above condition should afford a reasonable quantitative measure of the third term of Eq. 1. The values of EFOE density are expressed in % for the sake of numerical convenience by normalizing the wave function (Ψ_{FMO}) to 100 (Eq. 2).

$$\text{EFOE density (\%)} = 100 \times \int \Psi_{\text{FMO}}^2 d\Omega \quad (2)$$

Based on the Salem and Klopman equation (Eq. 1)¹¹ and the second-order perturbation theory²⁵ at the extended Hückel level,²⁶ a simple linear correlation between the EFOE density and activation enthalpy (ΔH^\ddagger) can be derived assuming that EFOE density should be proportional to the overlap integral (S) between reactant FMO's. Since the frontier orbital interaction energy (ΔE) between hydride HOMO and ketone LUMO is proportional to the square of the overlap integral between these FMO's, and this

interaction occurs in one face of the carbonyl plane, assuming that the overlap integrals between the reagents (S_a and S_b) should be linearly dependent on the respective π -plane-divided EFOE density (EFOE(a) and EFOE(b)), one obtains the following equation, which describes the linear relation between λ ($= \text{EFOE}(a)^2 - \text{EFOE}(b)^2$) and $\Delta\Delta H^\ddagger$ (facial difference in activation enthalpy: $\Delta\Delta H^\ddagger(b) - \Delta\Delta H^\ddagger(a)$) (Eq. 3).

$$\Delta\Delta H^\ddagger = m\lambda + n \quad (m > 0; n : \text{a constant}) \quad (3)$$

For a graphical plot of Eq. 3, natural log of observed stereoselectivity (product ratio) may be used if experimental $\Delta\Delta H^\ddagger$ is not available. We have previously observed an excellent linear correlation ($r^2 = 0.940$) for the NaBH_4 reduction of ten alkyl-substituted cyclohexanones including compounds with high steric hindrance.¹⁰ This equation has been successfully used for various other cyclic ketones, such as 3- or 4-substituted cyclohexanone⁷ and 5-aryladamantanones⁸ but was not applied in the present work.

Computational Methods

Spatial integration is limited to 5 au (2.65 Å) from molecular surface, where extension of the electronic wave functions is negligible beyond this limit. The carbonyl plane is defined as the plane which includes both sp^2 atoms of the π -bond (C=O) and which is parallel with the vector connecting the two carbon atoms at the α -positions (C1 and C3). Bondi's van der Waals radii²² were employed for the definition of molecular surface. The calculation procedure usually begins with structure optimization at the HF/6-31G(d) level using Gaussian 94 followed by a single point calculation with "ginput" and "pop=full" keywords at the same level.²⁷

The computer program was designed so that simultaneous calculation of both PDAS and EFOE density could be performed according to the three-dimensional lattice method with a unit lattice volume of 0.008 au³ ($1.18 \times 10^{-3} \text{ \AA}^3$). The quality of each EFOE calculation was checked by the value of the total electron density, which converged nearly unity (1.000 ± 0.001). All ab initio MO calculations were carried out with GAUSSIAN 94²⁷ on a UNIX computer workstation.

Application of the EFOE Model

Table 4 shows the EFOE analysis using the $\pi_{\text{C=O}}^*$ orbitals of the 1,3-diheteran-5-one series along with experimental stereoselectivities including the recent results of **1c**.²⁸ Both the EFOE density and the PDAS value predict correctly the experimentally observed stereochemical reversal of compounds **1a** and **2a**. In particular, the π -facial differences in the PDAS values between these substrates are significant, clearly indicating that the steric environment around the carbonyl carbons of these ketones (**1** and **2**) is opposite with each other. This is quite surprising because the two heteroatoms belonging to the same family in the periodic table exhibit exactly the opposite conformational property around the carbonyl.

Figure 7 depicts the side views of the conformations and the LUMOs of **1b** and **2b** optimized at the HF/6-31G(d) level. It is seen that the conformation of **1b** around the carbonyl is nearly planar (torsion angle along O=C5-C6-O1; $\tau = 158.5^\circ$) compared with cyclohexanone (torsion angle along O=C1-C2-C3; $\tau = 131.4^\circ$). The ring-flattening causes the enormous steric relaxation at the axial face (PDAS in the axial region = $\sim 70 \text{ au}^3$). In contrast, the geometry of **2b** around the carbonyl is significantly puckered (torsion angle along O=C5-C6-S1; $\tau = 115.9^\circ$), which leads to considerable increase in the PDAS values at the equatorial face ($\sim 55 \text{ au}^3$). The PDAS values for the *ax*-face of **2** ($\sim 18 \text{ au}^3$), which lack the axial hydrogens at the 1- and 3-positions, are nearly the same as the axial PDAS of cyclohexanone (19.4 au^3). The LUMO of **1b** is

more expanded into the *ax*-face than in the equatorial region, where significant out-of-phase (antibonding) contribution at H4_{ax} and H6_{ax} is observed with negligible contribution from the lone-pair orbitals in the *ax*-face. In sharp contrast, the LUMO of **2b** shows significant antibonding contribution of the high-lying lone pair orbitals in the *ax*-face with nearly zero contribution at H4_{ax} or H6_{ax} in the *eq*-face.

Table 4. EFOE analysis of **1** and **2** and observed diastereoselectivity (*ax* : *eq*).^a

Compd.	EFOE Density (%) ^b		PDAS (au ³) ^c		δ (%) ^d	Obs. (%)		
	<i>ax</i>	<i>eq</i>	<i>ax</i>	<i>eq</i>		Compd.	Reagent	<i>ax</i> : <i>eq</i>
1a ^e	1.279	0.245	67.6	26.5	40.7	1a ^f	LiAlH ₄	94 : 6
1b	1.739	0.243	71.2	26.2	40.4	1a ^f	RMgI ^h	96~98 : 4~2
1c	1.750	0.241	70.2	26.2	40.2	1c ^g	LiAlH ₄	89 : 11
						1c ^g	NaBH ₄	97 : 3
2a ^e	0.299	0.882	17.9	55.4	-17.1	2a ^f	LiAlH ₄	15 : 85
2b	0.277	0.834	18.4	54.6	-20.5	2a ^f	RMgI ^h	7~11 : 93~89
2c	0.278	0.854	19.0	54.1	-14.2			

^a Calculated at the HF/6-31G(d) level using the EFOE program¹⁰ after structure optimization with Gaussian 94²⁷ at the same level. ^b π -Plane-divided exterior frontier orbital electron density. ^c π -Plane-divided accessible space. ^d Orbital distortion index.²⁹ Positive sign indicates distortion toward the axial direction. ^e LUMO+2. ^f Ref. 12 and 14. ^g Ref. 14. ^h R = Me, *iso*-Pr, *tert*-Bu.

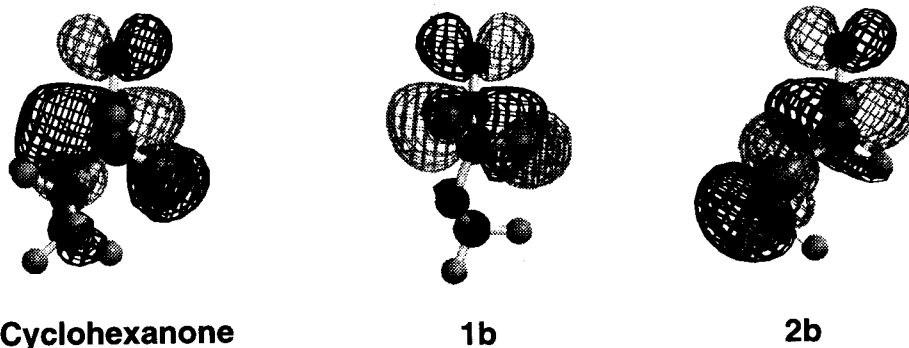


Figure 7. Side views of the LUMOs of cyclohexanone, **1b**, and **2b** (HF/6-31G(d)).

The EFOE data are consistent with the experimental facial stereoselectivity of sterically demanding Grignard reagents, such as *iso*-PrMgI, which shows nearly the same selectivity as hydride reduction. It is evident from Table 4 that these theoretical results should not be affected by the substituent at C2 (Ph, H, or *tert*-Bu) in 1,3-diheteran-5-ones. It is therefore concluded that marked conformational differences should be responsible for the reversal of facial stereoselection in these cases.

CONCLUSIONS

Origin of Conformational Deformation

Based on the above arguments, it may be reasonable to ascribe the origin of facial diastereoselection to the uniqueness of the ground state properties of **1** and **2** including their conformations rather than to the transition state effects. Figure 8 shows the side views of **1b** and **2b** along with two 1,3-diheteran-5-ones containing the heavier chalcogen atoms. Their structures were optimized at the HF/6-31G(d) level using Huzinaga basis for Se and Te.³⁰ One may immediately notice that their six-membered rings are more folded

on going from left to right. The ϕ values (the angle between the carbonyl plane and the plane containing X1, X3, C4 and C6) steadily increase on going from light to heavy chalcogenides (156.6°, 123.1°, 116.4° and 110.4° for O, S, Se, Te, respectively). In consonant with such a trend, the PDAS values over the axial face of the carbonyl plane steadily decrease (71.2, 18.4, 10.4, and 6.3 au³ for O, S, Se, Te, respectively). The mechanism of conformational deformation of six-membered rings containing heteroatom(s) is commonly attributed to changes in bond angles and lengths owing to the unique covalent properties of heteroatoms.²⁰ However, in the presence of a functional group possessing low-lying local LUMO such as carbonyl, another factor that affects significantly the conformation of the system may become important, since electron delocalization which occurs *via* vacant local molecular orbital(s) (MO)²⁴ is greatly facilitated by the presence of both low-lying unoccupied local MO(s) and nearby high-lying occupied MO(s). Since the order of the latter for the four heterocycles depicted in Figure 7 is $\sigma_{\text{CTe}} > \sigma_{\text{CSe}} > \sigma_{\text{CS}} > \sigma_{\text{CO}}$, it is expected that the hyperconjugative stabilization between these orbitals and carbonyl orbital may play an important role on molecular conformation.

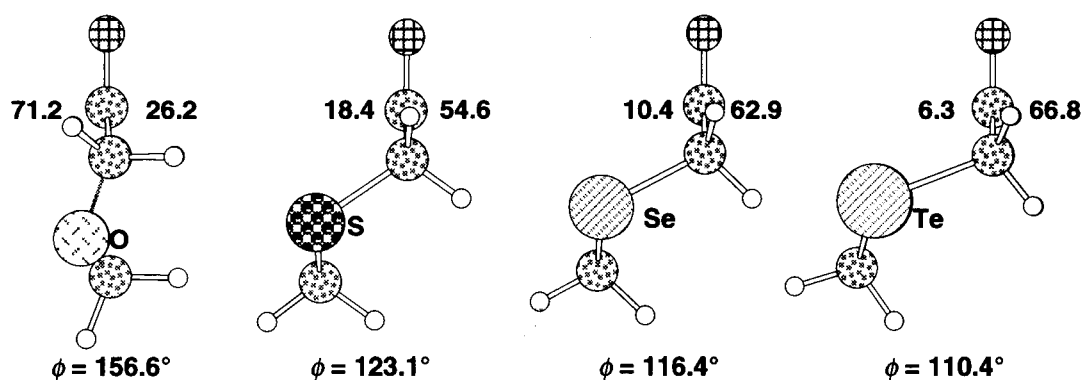


Figure 8. Side views of 1,3-diheteran-5-ones (heteroatom = O, S, Se, Te) optimized at the HF/6-31G(d) level. ϕ denotes the folding angle between the carbonyl plane and the X1-X3-C4-C6 plane. Numerical values indicated in the structures are PDAS in au³.

Table 5 shows the results of an NBO analysis of four analogs of 1,3-diheteran-5-ones (heteroatom = O, S, Se, Te). One may notice significant hyperconjugative electron delocalization around the carbonyl π bond. Two sets of such mechanisms, the Cieplak mode and the Felkin-Anh mode, are considered. Each of them is further classified into two mechanisms. As clearly seen in this Table, the oxygen heterocycle (**1b**) prefers the hyperconjugation between σ_{C4H4ax} and $\pi_{\text{C=O}}$, whereas the heavier heterocycles prefer the hyperconjugation between σ_{X3C4} and $\pi_{\text{C=O}}$.

Table 5. Antiperiplanar hyperconjugation involving the $\pi_{\text{C=O}}$ orbital in 1,3-diheteran-5-ones (heteroatom = O, S, Se, Te) (kcal mol⁻¹).^a

Heteroatom	Cieplak Mode		Felkin-Anh Mode	
	$\sigma_{\text{C4H4ax}} \rightarrow \pi_{\text{C=O}}^*$	$\sigma_{\text{X3C4}} \rightarrow \pi_{\text{C=O}}^*$	$\pi_{\text{C=O}} \rightarrow \sigma_{\text{C4H4ax}}^*$	$\pi_{\text{C=O}} \rightarrow \sigma_{\text{X3C4}}^*$
O	7.65	0.49	1.39	0.92
S	4.26	5.34	1.48	2.64
Se	3.01	8.51	1.18	3.04
Te	2.22	12.25	0.50	2.84

^a RHF/6-31G(d). Huzinaga basis sets were employed for Se and Te with diffuse functions for d-orbitals.³⁰

In addition, the Cieplak modes predominate over the Felkin-Anh modes irrespective of heteroatom. It is strongly suggested that hyperconjugative stabilization involving the carbonyl π orbital may be responsible for ground state conformational changes.

In conclusion, the importance of the ground state conformational difference between **1b** and **2b**, which should affect both the PDAS and the EFOE density values, has been demonstrated as the origin of π -facial diastereoselection in these heterocyclic systems as well. It is strongly suggested that transition state effects are not essential to π -facial diastereoselection in the present cases as well.

ACKNOWLEDGEMENTS

It is a great pleasure for the authors to join the special occasion of 73rd birthday celebration of Professor T. Mukaiyama by contributing their recent theoretical work on heterocyclic compounds, a part of which has been summarized by ST in a recent review article.⁵ Professor Mukaiyama's ingenious work in organic synthesis has always been a stimulus guide to ST since his graduate days. We thank Professor K. Fukumoto for inviting us to this magnificent occasion. Finally we thank Dr. Michio Iwaoka for computational assistance. We also express our special gratitude to the Ministry of Education, Science, Culture and Sports for financial support through Grants-in Aids for Scientific Research (Project Nos. 09440215 and 09239207).

00.

NOTES AND REFERENCES

1. *Chem. Rev.* Special Issue on 'Diastereoselection', B. W. Gung and W. J. le Noble, Ed. 1999, **99**, 1067.
2. A. S. Cieplak, *J. Am. Chem. Soc.*, 1981, **103**, 4540.
3. Y. D. Wu and K. N. Houk, *J. Am. Chem. Soc.*, 1987, **109**, 908.
4. M. Chérest and H. Felkin, *Tetrahedron Lett.*, 1968, 2205; M. Chérest, H. Felkin, and N. Prudent *Tetrahedron Lett.*, 1968, 2199; N. T. Anh, O. Eisenstein, J. M.-. Lefour, and M. E. Tran Huu Dau, *J. Am. Chem. Soc.*, 1976, **95**, 6146; N. T. Anh and O. Eisenstein, *Nouv. J. Chim.*, 1976, **1**, 61.
5. S. Tomoda, *Chem. Rev.*, 1999, **99**, 1243.
6. S. Tomoda and T. Senju, *Chem. Commun.*, 1999, 423.
7. S. Tomoda and T. Senju, *Tetrahedron*, 1999, **55**, 3871.
8. S. Tomoda and T. Senju, *Tetrahedron*, 1999, **55**, 5303.
9. A. E. Reed, L. A. Curtiss, and F. Weinhold, *Chem. Rev.*, 1988, **88**, 899. NBO program ver. 4.0 was used throughout this work.
10. S. Tomoda and T. Senju, *Tetrahedron*, 1997, **53**, 9057.
11. G. Klopman, *J. Am. Chem. Soc.*, 1968, **90**, 223; L. Salem, *J. Am. Chem. Soc.*, 1968, **90**, 543; I. Fleming, 'Frontier Orbitals and Organic Chemical Reactions', John Wiley & Sons, London, 1977.
12. J. C. Jochims, Y. Kobayashi, and E. Skrzewski, *Tetrahedron Lett.*, 1974, 571.
13. D. C. Wigfield and D. J. Phelps, *J. Am. Chem. Soc.*, 1974, **94**, 543; D. C. Wigfield and D. Phelps, *J. Org. Chem.*, 1976, **41**, 3789.
14. Y. M. Kobayashi, J. Lambrecht, J. C. Jochims, and U. Burkert, *Chem. Ber.*, 1978, **111**, 3442.
15. Y-D. Wu and K. N. Houk, *J. Am. Chem. Soc.*, 1987, **109**, 908.
16. Y-D. Wu, K. N. Houk, and M. N. Paddon-Row, *Angew. Chem.*, 1992, **104**, 1087; *Angew. Chem. Int. Ed. Engl.*, 1992, **31**, 1019; Y-D. Wu and K. N. Houk, *J. Am. Chem. Soc.*, 1993, **115**, 10992.
17. Percent Bond Elongation (%BE) = $(\Delta r / r_s) \times 100$, where Δr = the difference in the bond lengths between the vicinal antiperiplanar (AP) bond in transition state (r_{TS}) and the corresponding bond of starting ketone (r_s); $\Delta r = r_{TS} - r_s$. Both structures were optimized at the B3LYP/6-31+G(d) level.

18. R. P. Feynman, *Phys. Review*, 1939, **56**, 340.
19. G. Frenking, K. F. Kohler, and M. T. Reez, *Angew. Chem., Int. Ed. Engl.*, 1991, **30**, 1146.
20. E. L. Eliel, S. H. Wilen, and L. N. Mander 'Stereochemistry of Organic Compounds', John Wiley & Sons, New York, 1994, p.695.
21. S. Winstein and N. J. Holness, *J. Am. Chem. Soc.*, 1955, **89**, 5562.
22. A. Bondi, *J. Phys. Chem.*, 1964, **68**, 441.
23. K. Ohno, S. Matsumoto, and Y. Harada, *J. Chem. Phys.*, 1984, **81**, 4447.
24. K. Fukui, 'Theory of Orientation and Stereoselection', Springer Verlag, Heidelberg, 1979; K. Fukui and H. Fujimoto, 'Frontier Orbitals and Reaction Paths', World Scientific: London, 1997.
25. A. Imamura, *Mol. Phys.*, 1968, **15**, 225; L. Libit and R. Hoffmann, *J. Am. Chem. Soc.*, 1974, **96**, 1370.
26. R. Hoffmann, *J. Chem. Phys.*, 1963, **39**, 1397.
27. Gaussian 94 (Revision D.1 and E.2); Gaussian, Inc., Pittsburgh, PA, 1997; M. J. Frisch, G. W. Trucks, M. Head-Gordon, P. M. W. Gill, M. W. Wong, J. B. Foresman, B. G. Johnson, H. B. Schlegel, M. A. Robb, E. S. Replogle, R. Gomperts, J. L. Andres, K. Raghavachari, J. S. Binkley, C. Gonzalez, R. L. Martin, D. J. Fox, D. J. Defrees, J. Baker; J. J. P. Stewart, and J. A. Pople
28. Y. Senda, H. Sakurai, and H. Itoh, *Bull. Chem. Soc. Japan*, 1999, **72**, 285.
29. Orbital distortion index (δ) at carbonyl carbon (C-1) for the LUMO is defined by the following equation; $\delta = 100 \times (d_A - d_E) / (d_A + d_E)$, where d_A and d_E represent integrated "electron densities" due to the carbonyl carbon wave functions of the LUMO for both sides (axial and equatorial region) of the carbonyl plane.¹⁰
30. S. Huzinaga, 'Gaussian Basis Sets for Molecular Calculations' Elsevier: Amsterdam, 1984.

Received, 19th October, 1999